

SUMMARY OF 1991-1992 PROJECTS

Naval Postgraduate School
Space Systems Academic Group
Monterey, California

Professor Brij N. Agrawal
Daniel Sakoda, Teaching Assistant

**HIGH TEMPERATURE
SUPERCONDUCTING INFRARED IMAGING
SATELLITE**

**B. Angus, J. Covelli, N. Davinic, J. Hailey, E. Jones, V.
Ortiz, J. Racine, D. Satterwhite,
T. Spriesterbach, D. Sorensen, C. Sortun, R. Vaughan,
and C. Yi**

Abstract

A Low Earth Orbiting platform for an infrared (IR) sensor payload is examined based on the requirements of a Naval Research Laboratory statement-of-work. The experiment payload is a 1.5-meter square by 0.5-meter-high cubic structure equipped with the imaging system, radiators, and spacecraft mounting interface. The orbit is circular at 509 km (275 nmi) altitude and 70° inclination. The spacecraft is 3-axis stabilized with pointing accuracy of $\pm 0.5^\circ$ in each axis. The experiment payload requires two 15-minute sensing periods over two contiguous orbit periods for 30 minutes of sensing time per day. The spacecraft design is presented for launch via a Delta II rocket. Subsystem designs include attitude control, propulsion, electric power, telemetry, tracking and command, thermal design, structure, and cost analysis.

Introduction

The high temperature superconducting infrared imaging satellite (HTSCIRIS) is designed to perform a space-based infrared imaging and surveillance mission. The design requirements originated from the Naval Research Laboratory through a statement-of-work. The spacecraft is designed for a 3-year life in low-Earth orbit at 509.3-km altitude and 70° inclination. The satellite operates in a sensing mode and a standby mode. The satellite is nadir

pointing during the sensing mode where the spacecraft body frame tracks the moving local vertical with a specified roll axis orientation. The system is designed for two 15-minute scans over two consecutive orbits for each 24 hours. During the sensing mode, 150 watts of power are required. The standby mode operates in a sun-tracking orientation where the solar arrays charge the batteries and the imaging payload faces away from the sun. The standby mode requires 100 watts.

Payload Description

The payload weighs 362.9 kg and has dimensions of 1.52 x 1.52 x 0.51 meters. The payload attaches to the spacecraft bus on one 1.52 x 1.52 meter square surface. The infrared (IR) telescope and associated radiators are mounted opposite the mating face. The IR telescope has a 4° x 4° field-of-view and is mounted at a 45° angle to the surface of the payload. The telescope has a hinged protective cover that opens approximately 50° after the satellite is deployed.

The entire cryogenic cooling system is contained within the payload, and is designed to maintain the infrared detector at 65° Kelvin during the sensing mode. The cryogenic refrigeration system is designed to replenish the cold reservoir of liquid nitrogen when not sensing. The mechanical portion of the cryogenic cooling system is not operated while in the sensing mode.

The orientation of the payload is continuously measured by an inertial measurement unit (IMU). The IMU is periodically updated through two star sensors which are mounted on the front (+x-axis) face of the payload. Finally, a data processor is included within the payload to format the infrared data for transmission.

Mission Requirements

Mission specifications were outlined in a statement-of-work (SOW) generated at the Naval Research Laboratory (NRL). The following table shows the specifications for the orbit, attitude control system, electric power system, command, and telemetry.

Table 1 Requirements

Design life	3 years
Orbit altitude	509.3 km
Orbit inclination	70°
Method of attitude control	3-axis stabilized
Pointing accuracy	±5° each axis
Slew time	90° in 15 minutes
Settling time	1 minute
Rate stability	0.003° per second
RF communication	
Low data transfer rate	16 kbits (minimum)
High data transfer rate	150 mbits
Bit error rate	10 ⁻¹¹ (Encrypted) 10 ⁻⁹ (Unencrypted)
Minimum elevation angle	10°
Link availability due to rain attenuation	99%
Maximum ground antenna diameter	20 feet
Electric power	
Sensing mode	150 watts
Standby mode	100 watts

Spacecraft Configuration

The spacecraft bus is a box-like structure, 1.524 m square by 1.016 m tall. The bus is required to provide a stable platform to orient the sensor for imaging and standby modes. It is also required to provide electric power, command uplink, telemetry downlink, as well as real time transmission of the imaging data. The bus is constructed around a cylindrical aluminum monocoque thrust tube attached to an aluminum monocoque conical adapter cone. The cone protrudes through the face opposite the payload (the bottom face) and provides the

interface to the launch vehicle. The thrust tube and adapter carry the spacecraft launch loads. Four aluminum honeycomb panels are attached to the thrust tube and cone, constituting the sides of the spacecraft. These panels act as mounting surfaces for equipment and provide radiating surfaces for thermal control of the bus. An additional panel is located along the payload mounting face and provides a mounting surface for the payload.

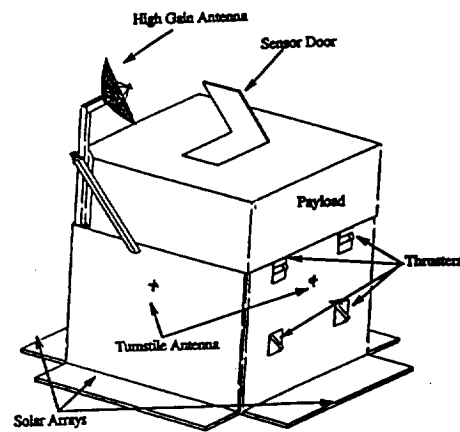


Fig. 1 Spacecraft configuration

Solar Arrays

Fixed solar arrays are located parallel to the bottom face and are mounted on panels that extend outboard from the bus. The arrays are 0.38 m wide by 1.47 m long. The silicon solar cells are mounted parallel to the anti-Earth face and are designed to provide maximum power to recharge the nickel hydrogen batteries as well as supply house-keeping power in the standby mode. The entire spacecraft power is provided by four rechargeable nickel-hydrogen batteries during the imaging mode.

Telemetry and Telecommand

Telemetry and communications are provided through one wide-band downlink antenna (WBDL), two omnidirectional transmit antennas, and two omnidirectional receive antennas. The omnidirectional transmit and receive antennas are paired on the pitch and anti-pitch faces to provide continuous telemetry and command capability. The WBDL antenna is gimbal-mounted to a boom that extends along one corner of the spacecraft, above the payload face, to allow horizon-to-horizon coverage during imaging revolutions. The support equipment, transmitters, receivers, and amplifiers are mounted interior to the bus. The high heat dissipating components are mounted to external panels. Two interior aluminum honeycomb panels provide mounting surfaces for the non-critical equipment. These equipment panels lie orthogonal to (and centered on) the axis of the conical adapter cone.

Attitude Control

Attitude control for the spacecraft is provided by four reaction wheels. Eight magnetic torque rods provide momentum desaturation. The reaction wheels are mounted near the top of the bus. Three of the wheels are inside the adapter cone with the fourth, the yaw wheel, inside the bus on the top of the uppermost equipment panel. Three of the wheels are oriented on mutually orthogonal axes with the fourth at a 45° angle from the other three. The torque rods are mounted, two per axis, on opposite side panels of the bus toward the top surface. Initial orbit correction and emergency attitude control (despin) are provided by eight 1-lbf hydrazine thrusters, mounted in groups of four on the pitch and anti-pitch faces of the bus. The thrusters are utilized as a backup to the primary attitude control system in addition to station keeping. The fuel and pressurant tank are located at the center of the adapter cone with the surface of the tank aligned with the top face of the bus.

Thermal Control

The thermal control system incorporates a passive design that maintains the bus and components at nominally low temperatures, and provides active heating to maintain temperatures within limits. The system is

composed of passive radiating and insulating material, applied to the surfaces of equipment and structures, and electric heaters attached to temperature sensitive components. Louvers are attached to the batteries as an additional measure to dissipate more heat energy.

Mass Summary

The following table depicts the mass properties of the subsystems.

Table 2 Mass summary

Subsystem	Mass
Payload	362.0 kg
T T & C	148.5 kg
Electric power	97.0 kg
Propulsion (dry)	8.3 kg
Attitude control	42.4 kg
Thermal control	24.8 kg
Structure	164.9 kg
Mechanical integration	73.3 kg
Subtotal	921.2 kg
Mass margin (20%)	184.2 kg
Propellant	12.9 kg
Total	1118.3 kg

Launch Vehicle

The launch vehicle is required to place the satellite in a circular orbit with a 509.3 km altitude and a 70° inclination. A Delta II (7320) launch vehicle was chosen for this mission. This launch vehicle is a two stage liquid-propelled rocket with three solid strap-on boosters. Typically a Delta II has nine solid strap-on boosters, but these are not required since this satellite has such a small mass.

Payload Envelope

The Delta II standard shroud is 2.184 m in diameter and 1.448 m high. It then expands to 2.54 m by 2.032 m. The payload has dimensions of 1.524 m x 1.524 m x 0.508 m. The necessary internal shroud diameter, therefore, is

2.155 m. The two-stage Delta II (7320) vehicle normally uses the 6019 attachment fitting. It weighs 57 kg and has a 1.524-m outer diameter at the attachment point.

Launch Sequence

The Delta II can be launched from either Cape Canaveral or Vandenberg AFB. Since the desired launch inclination is 70° , a West Coast launch is the best choice. The Delta II for this spacecraft will be launched from Vandenberg pad SLC-2W at a 158° launch azimuth.

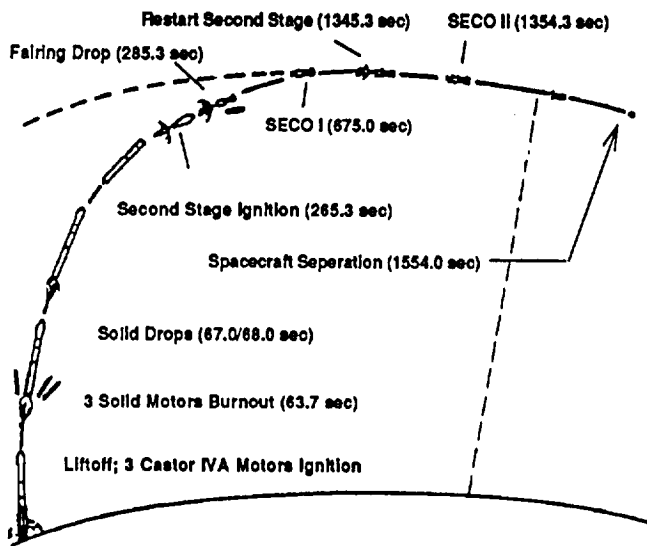


Fig. 2 Delta II launch sequence

The Delta II (7320) has two liquid stages as well as three solid strap-on boosters. The first stage RS-27 engine and the three solid rocket boosters are ignited on the ground at lift-off. Following burnout of the solids, the spent cases are jettisoned about one second later. The RS-27 engine continues to burn until main engine cutoff (MECO). This takes approximately 255 seconds.

After a short coast period, the first-to-second-stage separation bolts are blown, followed by second stage

ignition approximately five seconds later. The next major event is the payload fairing separation, which occurs early in the second stage flight.

The second stage burns for approximately 410 seconds, at which time stage two engine cutoff (SECO 1) occurs. The vehicle then follows a Hohmann transfer trajectory to the desired Low Earth Orbit altitude. After SECO 1 occurs, approximately 670 seconds later, the second stage is re-ignited and completes its burn to circularize the orbit. Satellite separation then begins approximately 200 seconds after stage two engine cutoff command (SECO 2).

Spacecraft Separation

The launch vehicle and the spacecraft are attached by three attachment bolts and bolt catcher assemblies. The separation sequence is described as follows.

"Upon separation, the bolts and catcher assemblies are retained by the spacecraft. . . . Following release of the three explosive nuts, the spacecraft/launch vehicle is stabilized by the launch vehicle attitude control system. Subsequently, three retaining latches are released followed by retrofire of the launch vehicle yielding a minimal separation tip-off of the spacecraft."¹

Fifteen seconds after the explosive bolts are fired, the latches are released. This delay allows the angular rates to dissipate. At this point the second stage retro-rocket fires providing the required relative separation velocity from the spacecraft. Expected angular velocities at separation are a little more than 0.2 degrees per second. This can be reduced by employing additional steps in the separation process. The angular velocity can be increased to 30 degrees per second (within a 5% accuracy) by using control jets.

Orbit Analysis

The infrared imaging mission dictates the orbital parameters for this spacecraft. These parameters were defined within the statement of work by NRL. The orbit requires 509.3-km altitude and a 70° inclination as summarized in the following table. The ground path of

this high inclination orbit yields maximum time over land masses and passes over the majority of the habitable land on the Earth. The characteristics of this orbit make the choice ideal to carry out successfully the mission of imaging a wide variety of targets with both land and water backgrounds.

Table 3 Orbit parameters

Parameter	Value
Apogee	6887.43 km
Perigee	6887.43 km
Period	1.58 hours
Inclination	70°
Arg. of Perigee	N/A
Long. of the asc. node	TBD (1)
Eccentricity	0.0
Altitude	509.3 km

(1) Longitude of ascending node determined by launch date

Orbital Perturbations

Orbital perturbations due to atmospheric drag, the Earth's oblateness, and effects from the Sun and moon were analyzed. The statement of work generated by NRL states that the allowable tolerance for altitude is 1.85 km (1 nmi) and 1° tolerance for inclination.

Altitude loss due to drag was calculated using the Artificial Satellite Analysis Program (ASAP) Version 2.0 developed by the Jet Propulsion Laboratory. The results indicate altitude loss at the rate of 4.50 km per year. This value was higher than the result from hand calculations and is used for propellant budget estimation.

Changes in inclination are attributed to the perturbations arising from the oblateness of the Earth and effects from the sun and moon. No cumulative effect on the inclination arises for this mission's circular orbit. The change in inclination due to the sun and moon were calculated and are presented in Figures 3 and 4. The maximum value for the effects due to the sun is 0.0084° per year. The maximum change in inclination due to the moon was found to be 0.023° per year.

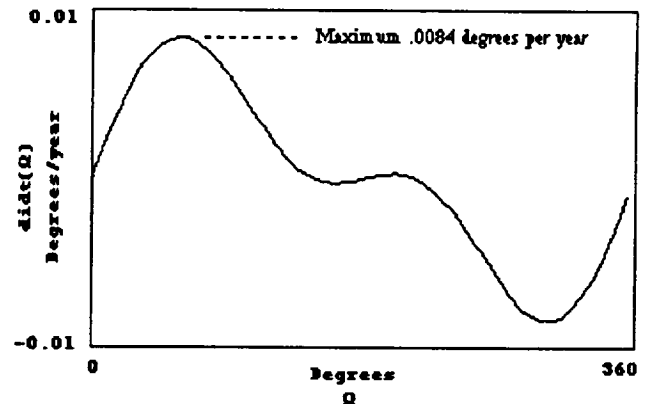
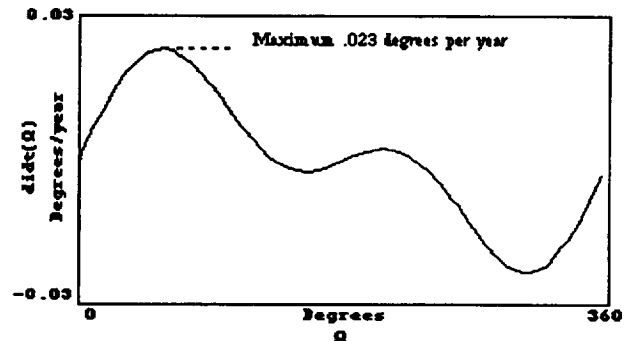


Fig. 3 Perturbation effects due to the sun

Fig. 4 Moon's influence on di/dt ($i_1 28 = 0.6^\circ$)

Effects in the longitude of the ascending node, Ω , were determined because inclination changes are a function of Ω . In addition, the longitude of the ascending node yields the daily ground track shift. The longitude of the ascending node shifts -2.6° per sidereal day. Each sidereal day, 15.14 orbits are completed, resulting in the orbit ground track shifting 0.84° East per 15 orbits.

Swath Width

The swath width of the spacecraft is required since transmission of the imaging data occurs simultaneously with imaging. This means that the receiving ground station must be in view while the spacecraft is scanning the target area. The footprint of the spacecraft's downlink is taken as 10° below the line-of-sight of the horizon. The result is a footprint whose angle is 65.7° subtended from nadir with respect to the spacecraft. The target object must be within a 90° scan of the spacecraft resulting in a $\pm 45^\circ$ angle from nadir with respect to the spacecraft.

The spacecraft, during the scan mode, adjusts the rate of roll to allow the fixed imaging payload to scan the target area. Simultaneously, a directional antenna is controlled to maintain contact with the ground station in view. The 509.3-km circular orbit defines the swath widths of 3165 km and 911 km for the ground stations and observation targets, respectively.

Subsystem Description

Communication, Telemetry, Tracking, and Command

The radio frequency communication subsystem (RFCS) is the interface between the satellite and the ground station. The RFCS includes the Command and Telemetry Subsystem (CATS), which provides the interface between the payload, spacecraft bus, and the ground station. As described in the statement of work, the Radio Frequency Communication Subsystem (RFCS) is required to provide the following capabilities:

- Omnidirectional command receive
- Omnidirectional low data rate (16 Kbps minimum) transmission
- Directional high data rate (150 Mbps maximum) transmission

The high-data-rate downlink system (HDRDS) is required to provide optimal spectrum usage for 150 Mbps with bit-error-rate of 10^{-11} encrypted and bit-error-rate of 10^{-9} unencrypted. The HDRDS is permitted a downlink with 99% availability due to rain attenuation. A minimum 10° elevation angle is required for data

collecting ground terminals. The ground station is assumed to have a 6-m (20 ft) diameter receive antenna.

A front-fed (symmetric) parabolic antenna was chosen for the High Data Rate Wide Band Downlink antenna design. Parabolic reflector antennas offer narrow beams over a wide range of frequencies. They are also simple to design and construct and have a proven performance record. For an offset parabolic antenna, the reflected beam is not intercepted by the feed horn which reduces the side lobes. The reduction in side lobes increases antenna efficiency.

The antenna sits on a boom extended from the spacecraft allowing a larger field of view. The antenna is gimballed to provide a wider range of pointing angles. The front-fed parabolic antenna will provide a 19- to 63-km diameter footprint with a 2.1 degree half-power beam width (HPBW). Antenna pointing control will consist of an open loop, onboard attitude and computer steer. This design provides $\pm 0.2^\circ$ of pointing accuracy with about 1 dB loss, assuming the attitude and control system maintains pointing within design tolerances. Using a closed-loop system would require the use of an auto-track receiver and a more complicated three-dimensional uplink beacon which must be constantly tracked. The additional cost and complexity of this system was not deemed necessary for this mission.

The principal objectives for spacecraft tracking, telemetry, and command (TT&C) are to provide information of operational use, failure analysis, and prediction of spacecraft performance. In routine operations, the telemetry verifies commands and equipment status and also alerts personnel of any unusual occurrences. Telemetry can also be used to analyze any degradation that might affect performance and predict its effect on spacecraft lifetime. The TT&C consists of two sets of omnidirectional turnstile antennas, Command and Data Handling system (C&DH) and the Air Force Satellite Control Network (AFSCN).

The turnstile antenna consists of two half-wave dipole antennas intersecting in the middle and at a 90° angle from each other. This provides the necessary 180° arrangement for near omnidirectional coverage. They extend from the plane of the spacecraft a distance of $\lambda/4$ (0.0375 m) for optimal gain out to $\lambda/2$ (0.075 m) for

minimal gain, where λ is the wavelength. Tables 4 and 5 summarize the communication and TT&C subsystems.

Table 4 Communication subsystem summary

Unit	Qty.	Length (cm)	Width (cm)	Height (cm)	Weight (kg)	Power (watts)
Downlink transmitter	2	16.7	7.6	17.3	3	22
Wide band transmitter	2	22.8	22.8	11.4	19	75
WBDL antenna	1				15	
Antenna actuator	1				4.5	5
Omni xmit antenna	2				1.7	5
Omni rcv antenna	2				1.6	5
Hybrid divider	2	5	5	0.6	0.25	
Receiver/demod	2	17.8	17.2	17.8	6.8	2
RFCS total:					51.85	114

Table 5 Command and telemetry subsystem summary

Unit	Qty.	Length (cm)	Width (cm)	Height (cm)	Weight (kg)	Power (w)
Data interface (DIU)	2	35.5	21.6	24.1	19.9	25
Remote interface (RIU)	2	24.4	23.1	24.9	29.9	6
Telem & command (TCU)	2	21.1	35.6	19	8.1	15
Uplink processor	2	9.9	14.2	11.7	3.6	9.5
Downlink processor	2	9.9	14.2	11.7	3.6	9.5
CATS Total:					65.1	65
Total Comm/TTC					116.95	179

Electric Power Subsystem

The satellite electrical power subsystem consists of four solar arrays that nominally generate 34.2V at 4.3A at end-of-life (EOL), four 10Ah NiH₂ batteries, and power conditioning equipment for a fully regulated bus at 28 V (± 4 V). Regulation is achieved by use of two partial shunt regulators on each solar panel and one series dissipative regulator at the battery discharge terminal. One of the partial shunt regulators on the panel regulates the voltage supplied to the housekeeping bus when that array is aligned as such. The other partial shunt regulator is used

to regulate the battery charging voltage, when the array is aligned for battery charging.

There are four arrays mounted in a stationary manner. Each array is capable of filling the role as either charge array or housekeeping array. Two arrays are normally required for battery charging and one for housekeeping. Each array is composed of seven parallel strings of 73 cells in series. The cells selected are 10 ohm, 0.02 cm thick, 2.5 cm x 6.2 cm silicon cells with back-surface reflector and TiO_xAl₂O₃ anti-reflective coating. The manipulation of the solar array's power distribution is done from ground control.

The batteries are designed to carry the electrical demand during eclipse and the additional load that arises during sensing and data transfer. Four 10Ah NiH₂ batteries are used. The batteries are designed to operate to a 60% depth-of-discharge (DOD). The batteries will have approximately 21 hours to recharge fully after reaching the 60% DOD.

Radiation degradation of the solar cells was calculated for the duration of the mission. The results on the cell parameters are depicted in Table 6.

Table 6 Radiation degradation of solar cells

	EOL	BOL
P _{MAX} (W)	148	158
V _{OC} (V)	42.8	44.4
I _{SC} (A)	4.69	4.74
I _{MP} (A)	4.34	4.36
V _{MP} (V)	34.2	36.6

Propulsion

The MR-111C 1-lbf thruster built by Rocket Research Company was chosen for this design. Table 7 gives the design and performance characteristics of the thruster.

Table 7 MR-111C Thruster characteristics

Propellant	Hydrazine
Catalyst	Shell 405
Steady state thrust (N)	5.338 - 1.334
Feed pressure (MPa)	2.7579 - 0.5516
Chamber pressure (MPa)	1.2066 - 0.3447
Expansion ratio	74:1
Flow rate (g/sec)	2.404 - 0.635
Mass (kg)	0.33113
Specific impulse (sec)	229 - 226
Minimum impulse bit (N-s)	0.0845 @ 2.4132 MPa & 20 ms On

The propulsion subsystem is required to perform on a primary basis detumbling of the spacecraft, spin-down,

and delta V maneuvers for orbit maintenance. The secondary requirements of the propulsion subsystem are to provide redundancy for desaturation of the reaction wheels, perform slew maneuvers, and deorbit.

Eight thrusters, located on the positive and negative roll face, are used. The thrusters are canted 35.8° off the normal to the face and oriented to thrust in the x-z plane. The canting of the thrusters provides a moment arm with components in the x, y, and z planes. Figure 5 shows the placement of the thrusters on one face.

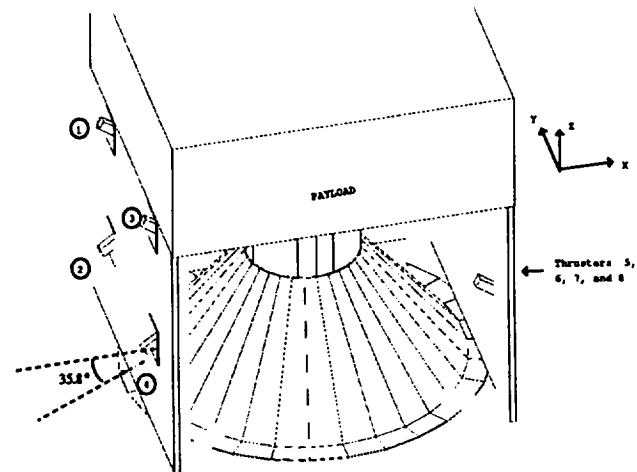


Figure 5 Thruster location and cant angle

The thruster numbers and locations are shown in Table 8, while the thruster operations are depicted in Table 9.

Table 8 Thruster placement

Thruster Number	Location ¹ (meters)	Moment arm ¹ (meters)	Moment created ¹ (N*m)
(1) anti-roll face	[-.762,-.427,-.241]	[-.146,-.427,.203]	[-1.11,1.11,1.54]
(2) anti-roll face	[-.762,-.427,.241]	[-.146,-.427,-.203]	[1.11,-1.11,1.54]
(3) anti-roll face	[-.762,.427,-.241]	[-.146,.427,-.203]	[1.11,1.11,-1.54]
(4) anti-roll face	[-.762,.427,.241]	[-.146,.427,-.203]	[-1.11,-1.11,-1.54]
(5) roll face	[.762,-.427,-.241]	[.146,-.427,.203]	[-1.11,-1.11,-1.54]
(6) roll face	[.762,-.427,.241]	[.146,-.427,-.203]	[1.11,1.11,-1.54]
(7) roll face	[.762,.427,-.241]	[.146,.427,.203]	[1.11,-1.11,1.54]
(8) roll face	[.762,.427,.241]	[.146,.427,-.203]	[-1.11,1.11,1.54]

¹Note: All distances are measured from the beginning-of-life center of mass for the spacecraft

Table 9 Thruster operations

Operation	Thruster number	Redundant
Orbital insertion	1, 2, 3, and 4	5, 6, 7, and 8
Atmospheric drag	1, 2, 3, and 4	5, 6, 7, and 8
Positive roll (+X)	2 and 3	7 and 6
Negative roll (-X)	1 and 4	8 and 5
Positive pitch (+Y)	2 and 4	7 and 5
Negative pitch (-Y)	1 and 3	8 and 6
Positive yaw (+Z)	1 and 2	8 and 7
Negative yaw (-Z)	3 and 4	6 and 5

The propellant budget is outlined in the following table.

Table 10 Propellant budget

Propellant for Δv maneuvers and control	11.03
Allowance for off-nominal performance	0.11
Allowance for off-nominal operations	0.11
Mission margin (reserves)	1.10
Contingency	1.10
Total required propellant	13.45
Residual propellant (trapped in motor case, tanks, lines, etc.)	0.27
Loading uncertainty	0.07
Total propellant load	13.79 kg

A survey was conducted of off-the-shelf positive expulsion tanks based on the above minimum fuel tank diameter and the diameter of the satellite cylinder ($\cong 0.5$ meters). The TRW 80225-1 sphere used by the OTS-Marex program was selected since it was the closest match in propellant capacity. The required tank diameter was determined to be 0.322 meters.

Attitude Control Subsystem

The choice of configuration was driven mainly by the requirements to be able to slew about multiple axes in varying geometries and to maintain reasonably accurate 3-axis stability. Adequate redundancy is crucial because

the ACS must be able to orient for both payload operations and power collection. Three orthogonal Reaction Wheel Assemblies (RWAs), one along each body axis, allow somewhat independent control of rotation about each axis. A fourth RWA is skewed 45° out of plane with respect to the others to back up any single RWA failure. In the event of an RWA failure, the redundant rate will be commanded $\sqrt{3}$ times the normal rate to achieve the desired effect while the undesired components are temporarily taken up by the other wheels.

Momentum dumping is accomplished by pairs of orthogonal magnetic torque rods. Normal operations call for the pairs to work simultaneously to rapidly desaturate the RWAs before slew maneuvers and to activate periodically to keep the RWA bias low. Specifically, automatic desaturation begins at 210 rpm. This minimizes dynamic coupling in the Euler equations. The rods can work singly in the event of a failure. Redundancy for momentum dumping is provided by the propulsion system, available in the event of complete torque rod failure. Both the magnetic dumping system and the propulsion system give limited three-axis stability in the event of multiple RWA failure.

Attitude errors are induced by solar, aerodynamic, gravity gradient, magnetic disturbance torques, and perturbations during desaturation and ΔV maneuvers. The two Attitude Control Computers (ACC) receive data from the IMU, the Earth sensor, one of two sun sensors in view, and the backup gyro assembly to compute and

store two sets of these errors: (1) the Euler angles with respect to the standard nadir pointing sensing coordinates and (2) the Euler angles with respect to the sun-tracking coordinates, which track the incoming sun vector and can be considered "inertially" fixed. From these, each computer can calculate the direction cosine matrix used in its duty slew direction. In the event of a single computer failure, the other assumes the load for both. The first set of errors includes the orbital rate, while the second set is fixed with respect to the orbit normal coordinate system. Twelve independent transformations exist in each case (sign ambiguities are removed), and the computer defaults to the one which results in the minimum total correction path (or slew path), but any specific direction cosine matrix can be chosen. The duty ACC then commands the RWAs to perform the chosen sequence of single-axis slews to reach the target axes (i.e., to zero the Euler angles). From here, smaller slews can be commanded to accomplish offset nadir pointing, or to correct a thermal problem. Single-axis slew sequences are not the fastest method, but they simplify constraint checking, allow separate orthogonal error computation, and minimize dynamic coupling.

The design of two primary controllers covers the operation of all the modes and will be discussed here: (1) the sensing mode controller and (2) the slew controller. Only subtle changes separate the controllers between sun-tracking and sensing mode, sun-tracking and ΔV mode, and slew and acquisition. The component selection summary is depicted in the Tables 11 and 12.

Table 11 ACS Sensors and electronics

Component	Mass (kg)	Power (w)	Manufacturer
Backup spring restraint gyro assembly	1.3	19.5	Heritage:DMSP
Precision pointing Earth sensor	3.8	4.0	Barnes
Attitude control computers (2)	2.5 ea	6.0 ea	MIL-STD-1750 (GPS Version)
Sun sensor (sense mode)	0.04	1.0	Adcole
Sun sensor (sun-track mode)	0.04	1.0	Adcole

Table 12 ACS Angular momentum devices

Component	Storage Capacity (Nms)	Peak Torque (Nm)	Mass (kg)	Power (w)	Manufacturer
Roll RWA	19.9	0.3	9.09	<140 Peak <10 Nom.	Honeywell
Pitch RWA	19.9	0.3	9.09	<140 Peak <10 Nom.	Honeywell
Yaw RWA	19.9	0.3	9.09	<140 Peak <10 Nom.	Honeywell
Redundant RWA	19.9	0.3	9.09	<140 Peak <10 Nom.	Honeywell
Torque rods (6)	N/A	.003 max @ 10Am ²	1.76 ea	1.6 ea	Ithaco

Thermal Control Subsystem

Thermal control of the spacecraft bus is achieved using a near passive thermal control system. Passive control systems are simpler, more reliable, and more cost effective than active systems. The most attractive of these features are the simplicity and reliability. Passive components of the system include optical solar reflectors (OSR), multi-layer insulation (MLI), temperature sensors, fiberglass standoffs, and space-qualified coatings/paints. Temperature sensors are used to control strip heaters located on critical elements. A pair of temperature sensor-controlled louvers are used for thermal control of the batteries. All items are generally readily available hardware.

Critical components are kept above their low temperature limits by applying heater power. The bus is equipped with 15 heaters that range in size from 2.5 w to 20 w. Spacecraft heaters are electrical resistance elements that are mounted directly to the exterior surface of the critical component. The heaters are controlled by a closed loop system that includes local temperature sensors. Although the heaters function autonomously, the provision has been made for ground controlled operation with availability of adequate telemetry channels.

The nickel-hydrogen batteries require a very narrow temperature range of 0° C to 10° C. The batteries were placed on the ±X panels with MLI on the interior of the spacecraft and louvers facing space. Additionally, the batteries are thermally decoupled from the rest of the spacecraft to eliminate spurious heat inputs from other components.

A thermal model was generated using the PC-ITAS® thermal analysis software by Analytix, Corp. The model used in the analyses consisted of 80 active nodes. Two orientations were studied: the Earth-sensing mode and the on-orbit standby mode. Results of the analysis are given in Table 13.

Table 13 Thermal analysis results

Component	Sensing min/max (°C)	Standby min/max (°C)
Payload/bus/interface	+3/+11	0/+30
Batteries	0/+13	0/+18
Fuel tank	-11/+10	-9/+29
Solar arrays	-57/+13	-44/+66
Antenna	-14/-13	-43/-27
ADCS electronics	-40/-10	-39/-10
TT&C electronics	-49/+91	-46/-14
EPS electronics	-37/+33	-46/+4
Reaction wheels	-40/-10	-39/-10

Structure Design

The primary load-carrying members for axial compressive loads and bending moments are the central cylinder and conical adapter. These are monocoque shells of 6061-T6 Aluminum designed to withstand the ultimate quasi-static loads during launch. The design loads used a factor of safety of 1.5 for the axial and lateral

limit loads of 7.2 and 2.5 g's of the Delta II launch vehicle. Aluminum 6061-T6 was chosen for its ease of machining and large strength-to-weight ratio.

The spacecraft is made up of seven aluminum honeycomb panels in addition to the cylinder and conical adapter. The top panel supports the load of the payload and transmits it to the central cylinder and cone. The two equipment panels support the subsystem components. The remaining panels make up the body of the spacecraft bus. The panels are designed for stiffness to meet the design criteria for a minimum natural frequency of 50 Hz and stress due to dynamic loads. The adapter ring transfers the loads from the conical section to the 6019 adapter of the Delta II. The frame of the spacecraft bus is made of aluminum square tubing. It provides the mounting surfaces for the side panels and the parabolic antenna.

A finite element analysis of the structure was done using the CASA/GIFTS Finite Element Analysis software on a MicroVAX 2000 cluster. Static analysis of the spacecraft was performed using the loads for the Delta II launch vehicle. The maximum translational deflection occurs at the tip of the antenna support. This deflection is only 1.2 mm. The maximum rotational deflection of 2.2 mm also occurs at this point. The maximum stress in the spacecraft is 87.9% of the maximum yield stress using Von Mises' yield criterion. This results in a margin of safety of 13.8%.

The finite element model was also studied for dynamic analysis. The requirement that the fundamental modal frequency be above 50 Hz was never satisfied. Due to time constraints, modifications to the structure design were not possible. The fundamental modal frequency was found to be 22.76 Hz.

Spacecraft Testing

The spacecraft test plan (Figure 6) promotes the use of "proto-flight" testing in accordance with the "USAF Military Standard Test Requirement for Space Vehicles (MIL-STD-1540B)." This is done in an effort to lower costs incurred in the testing phase. A test model is used for dynamic testing and thermal balance. A full vehicle is then built to flight standards and undergoes system level testing and is used as the flight unit.

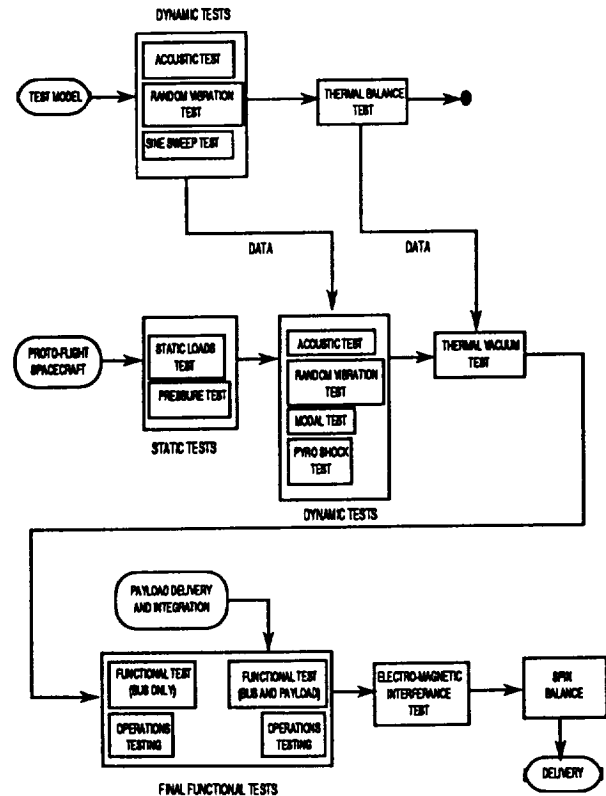


Fig. 6 Spacecraft testing flow diagram

Component level testing will be done for functionality and for random vibration. The components selected are all flight-qualified with validated quality. Once attached to the flight vehicle, the components will undergo all system level testing.

The test model will be fitted with mass and electrical simulation components. The test model is used for acoustic, random vibration, sine sweep, and thermal balance testing. The data gained is used in the component testing as well as the system level testing.

System level testing includes static load, pressure, acoustic, random vibration, modal, pyro shock, and thermal vacuum testing for environment compatibility.

Functional testing will be performed for mechanical devices, interface fittings, and operating limits. Functional testing will also be done for electrical performance.

Cost Analysis

A cost analysis of the spacecraft development and launch was done using the "Unmanned Space Vehicle Cost Model," Revision 6 (USCM6). The USCM6 is a parametric estimating tool. Mathematical expressions are derived relating cost as the dependent variable of selected independent cost driver variables. These relationships are derived by statistically correlating the historical cost data of several related or similar systems to physical and/or performance characteristics of those same systems. This approach assumes that the driving forces that affected cost in the past will continue to affect cost in the future. Table 14 presents the cost analysis summary.

Table 14 Cost analysis summary (millions \$)

Category	Most Likely	Low Est.	High Est.
Satellite	73.43	47.97	98.88
Launch	39.1	39.1	39.1
Program level	29.59	22.68	36.5
Aerospace ground equipment	9.64	7.14	12.15
Launch & Orbital Ops Support (LOOS)	3.53	2.71	4.36
Total	155.29	119.6	190.99

Conclusion

A spacecraft design is presented to provide mission support for the High Temperature Superconductor Infrared Imaging payload. The requirements were outlined in a statement-of-work generated by the Naval Research Laboratory. A preliminary design was done as part of the AE 4871 Advanced Spacecraft Design course during the Fall quarter. Due to time constraints,

deficiencies in the structure design could not be corrected. An additional deficiency arose due to neglect of the interaction between the antenna slew and the attitude control maneuver for spacecraft slew.

Acknowledgments

The design team would like to thank Professor Brij Agrawal for his guidance and assistance throughout the quarter. We also wish to thank Professor Edward Euler and Mr. Dan Sakoda of NPS for their invaluable help. Dr. Alan Schaum, George Price, Woody Ewen, Nelson Hyman, and Porter Lyon of the Naval Research Laboratory provided valuable insight into all facets of the satellite design. Finally, we appreciate the continued interest and support of Dr. Kim Aaron, our NASA/USRA representative at the Jet Propulsion Laboratory.

References

1. Angus, B. et al. Spacecraft Design Project, High Temperature Superconducting Infrared Imaging Satellite, Naval Postgraduate School, December 1992.
2. Commercial Delta II Payload Planners Guide, MDC H3224B, December 1989, pp. 3-5.
3. Agrawal, B.N. Design of Geosynchronous Spacecraft, Prentice-Hall: New York, 1986.
4. Solar Cell Array Design Handbook, JPL Publication SP43-38, Volumes 1, 2, and 3, October 1976.
5. Wertz and Larson. Space Mission Analysis and Design, Kluwer Academic Press, 1989.
6. Space Division Unmanned Space Vehicle Cost Model, 6th Edition, Space Division Report Number: SD TR-88-97, November 1988.